Dalton Transactions

PAPER

View Article Online
View Journal

Check for updates

Cite this: DOI: 10.1039/c9dt01802f

Photolysis of Tp'Rh(CNneopentyl)(PhNCNneopentyl) in the presence of ketones and esters: kinetic and thermodynamic selectivity for activation of different aliphatic C–H bonds†‡

Astrid M. Parsons and William D. Jones *

Received 29th April 2019,
Accepted 24th May 2019

DOI: 10.1039/c9dt01802f

rsc.li/dalton

The active fragment [Tp'Rh(CNneopentyl)], generated from the precursor Tp'Rh(CNneopentyl)(PhN=CNneopentyl), underwent oxidative addition of substituted ketones and esters resulting in Tp'Rh(CNneopentyl)(R)(H) complexes (Tp' = tris-(3,5-dimethylpyrazolyl)borate). These C–H activated complexes underwent reductive elimination at varying temperatures (24–70 °C) in C_6D_6 or C_6D_{12}. Using previously established kinetic techniques, the relative Rh–C bond strengths were calculated. Analysis of the relative Rh–C bond strengths *vs.* C–H bond strengths shows a linear correlation with slope $R_{M-C/C-H}$ = 1.22 (12). In general, α-substituents increase the relative Rh–C bond strengths compared to the C–H bond that is broken.

Published on 27 May 2019. Downloaded by Nottingham Trent University on 6/6/2019 1:24:10 AM.

Introduction

Transition metal-based strategies for C–H functionalization have revolutionized the field of organic chemistry. In particular, C–H functionalization processes can enable for the efficient synthesis of biologically and pharmaceutically relevant molecules and feedstock commodity chemicals.[1] One major challenge for the activation and functionalization of C–H bonds is the ability to control regioselectivity. Often, modifications to the ligand scaffold provide a means to alter selectivity for different C–H bonds. Therefore, a detailed understanding of the underlying effects of ligand choice on selectivity for C–H activation would allow for the rational design of efficient catalytic systems.

In general, the process of oxidative addition of C–H bonds to coordinatively unsaturated metal centers is photochemically or thermally initiated. A number of early studies of C–H activation revealed the relative thermodynamic stabilities of products formed *via* oxidative addition to unsaturated metal centers[2] and, from these, the relative metal–carbon bond strengths could be determined.[3] Our lab found that the relative thermodynamic stability (ΔG°) can be determined experimentally by the thermodynamic cycle shown in Fig. 1.[4] These derived thermodynamic stabilities can be combined with the known C–H bond strengths to provide relative metal–carbon bond strengths, which are useful for interpreting the factors that contribute to product distributions. Related methods to measure these energetic parameters have been applied by Wolczanski to $(^tBu_3SiO)_2(^tBuSiNH)Ti(R)$[5] (R = alkyl, aryl, benzyl, and vinyl groups) and $(^tBu_3NH)_2(^tBu_3\text{-}SiN{=})Ta(R)$[6] (R = Ph, Me, benzyl) systems, where a linear correlation between M–C and C–H bond energies was observed with slope $R_{M-C/C-H}$ = 1.1 and 1.0, respectively.

In a similar study, Bercaw observed a trend with $R_{M-C/C-H}$ = 1.29 for Cp^*_2Sc-R complexes (R = alkyl, phenyl, alkynyl).[7] Bryndza and co-workers have shown linear 1 : 1 relationships

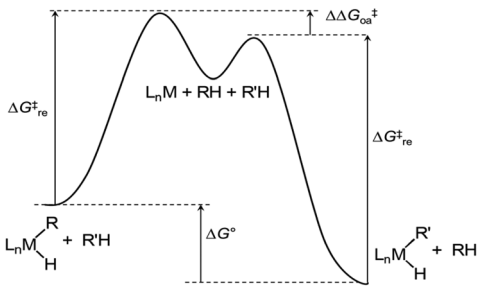

Fig. 1 Free energy diagram for competitive C–H activation.

Department of Chemistry, University of Rochester, Rochester, New York 14627, USA. E-mail: jones@chem.rochester.edu

†This paper is dedicated to our collaborator and friend Prof. Robin Perutz FRS on the occasion of his 70th birthday, in recognition of his many important and creative contributions to C–H bond activation.

‡Electronic supplementary information (ESI) available: Experimental procedures and characterization data for all reactions. DFT calculated C–H bond strengths. See DOI: 10.1039/c9dt01802f

Published on 27 May 2019. Downloaded by Nottingham Trent University on 6/6/2019 1:24:10 AM.

between M–X and H–X bond strengths for two different systems, $Cp^*Ru(PMe_3)_2(X)$ and (dppe)Pt(Me)(X), where X is OH, OR, NR_2, PR_2, SiR_3, and SH.[8] These correlations appear to be unaffected by steric differences. Marks also noted a nearly linear correlation of Zr–X and Hf–X bond strengths with X–H bond strengths.[9]

Eisenstein and Perutz have examined the above titanium and Tp′Rh systems computationally, where both M–C and C–H bond strengths can be calculated using DFT. They found reasonably good correlations for the substrates examined (all hydrocarbons), with the exception of benzyl and allyl, which lay above the correlation line.[10] They also found good correlations with slopes in the range 1.9–3.0 for the activation of polyfluoroarenes with a variety of metal complexes (Zr–Ni).[11] Landis has also summarized and compared a number of systems where some correlation between M–X and X–H (X includes C) bond strengths has been observed.[12]

Our group has been interested in studying the effect of common organic functional groups on C–H activation reactions using the [Tp′Rh(CNneopentyl)] fragment, which is cleanly generated by irradiation of Tp′Rh(CNneopentyl)(PhNCN-neopentyl) **1**. We have discovered that activation of 1-chloropentane and 3-chloropentane results in exclusive C–H activation of the terminal methyl groups.[13] When examining the activation of 2-chloropentane, a mixture of 4-chloropentyl activation product and Tp′Rh(CNneopentyl)HCl arising from β-chloride elimination of the 2-chloropentyl activation product was observed. Studying the activation of various 1-chloroalkanes (C_1–C_5) revealed that chlorine substituents have a dramatic effect on the stabilization of the resulting alkyl hydride species formed.[14] In a separate study, it was concluded that reductive elimination of hydrocarbons featuring α-cyano substituents required elevated temperatures.[15] The observed stabilization effect was attributed not to the strengthening of the Rh–C bond due to the electron withdrawing character of the cyano group, but rather to the formation of a weak α-cyano C–H bond in the transition state for reductive elimination. More recently, it was concluded that aryl, vinyl, alkynyl, alkoxy, CN, and keto α-substitution on Rh-methyl complexes results in a weakening of the Rh–CH_2X bond compared to the Rh–methyl bond.[16] However, when considering the relative C–H bond strengths (methane *vs.* H–CH_2X), it is clear that substituents have a positive effect on strengthening the metal–carbon bond. Given these results and in view of the importance of ketones and esters as building blocks, we became interested in further understanding how substitution on a variety of simple ketones and esters affects selectivity for C–H bond activation.

Results and discussion

C–H activation of ketones

Irradiation of Tp′Rh(CNneopentyl)(PhNCNneopentyl) (**1**) provides access to the coordinatively unsaturated fragment [Tp′Rh(CNneopentyl)] which readily reacts with most hydrocarbons giving rise to C–H oxidative addition products.[17] Previously, it was shown that photolysis of **1** in neat acetone results in the clean formation of Tp′Rh(CNneopentyl)($CH_2C(=O)CH_3$)(H) with a hydride doublet at δ −14.78 featuring a small rhodium–hydride coupling constant (d, J_{Rh-H} = 19.8 Hz).[16] No evidence for an O-bound enolate was observed. In this prior report, only this one example of ketone activation was reported. Herein, we investigate the activation of substituted ketones and esters by rhodium complex, **1**. Scheme 1 summarizes the major products in the reactions with ketones.

Photolysis of **1** in neat diethyl ketone **2a** results in a color change from bright to pale yellow after 15 minutes at 0 °C. ^{1}H NMR spectroscopic analysis of the reaction mixture in C_6D_6 reveals the formation of one major species, Tp′Rh(CNneopentyl)($CH_2CH_2C(=O)CH_2CH_3$)(H) (**3a**), with a hydride resonance at δ −14.89 (d, J_{Rh-H} = 24.0 Hz) (Scheme 1). This magnitude of a Rh–H coupling constant is typical for unsubstituted alkyl hydride species, indicating activation of a methyl C–H bond rather than an α-keto C–H bond activation.[4] Small quantities of *o*-, *m*-, and *p*-carbodiimide activation products are also observed as 3 doublets near δ −13.40 and −13.70. The ^{1}H NMR spectrum of the hydride region also shows small

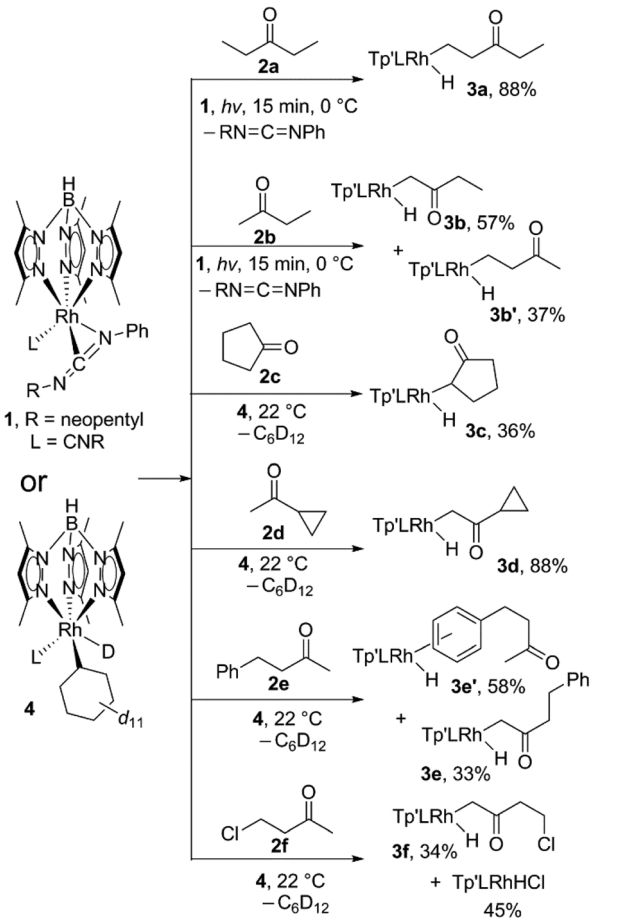

Scheme 1 Major products from reaction of [Tp′Rh(CNR)] with various ketones.

This journal is © The Royal Society of Chemistry 2019

Published on 27 May 2019. Downloaded by Nottingham Trent University on 6/6/2019 1:24:10 AM.

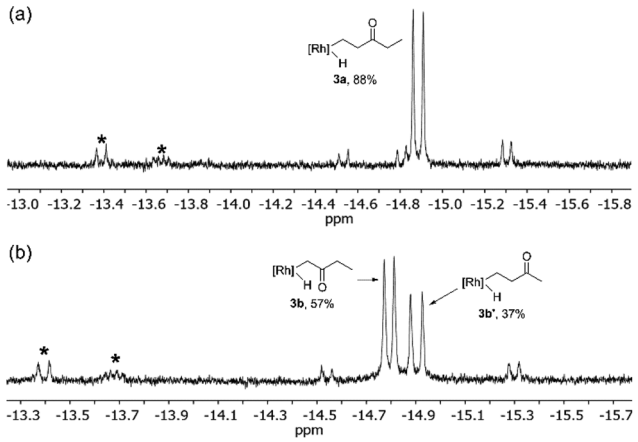

Fig. 2 ^{1}H NMR spectrum (500 MHz) of the hydride region of the reaction of **1** with (a) diethyl ketone and (b) methyl ethyl ketone. All spectra recorded in C_6D_6. * indicates *o*-, *m*-, and *p*-carbodiimide activation products. The small doublet at δ −14.81 (J_{Rh-H} = 19.9 Hz) in (a) is assigned to C–H activation of a trace impurity in the diethyl ketone (*e.g.*, acetone).

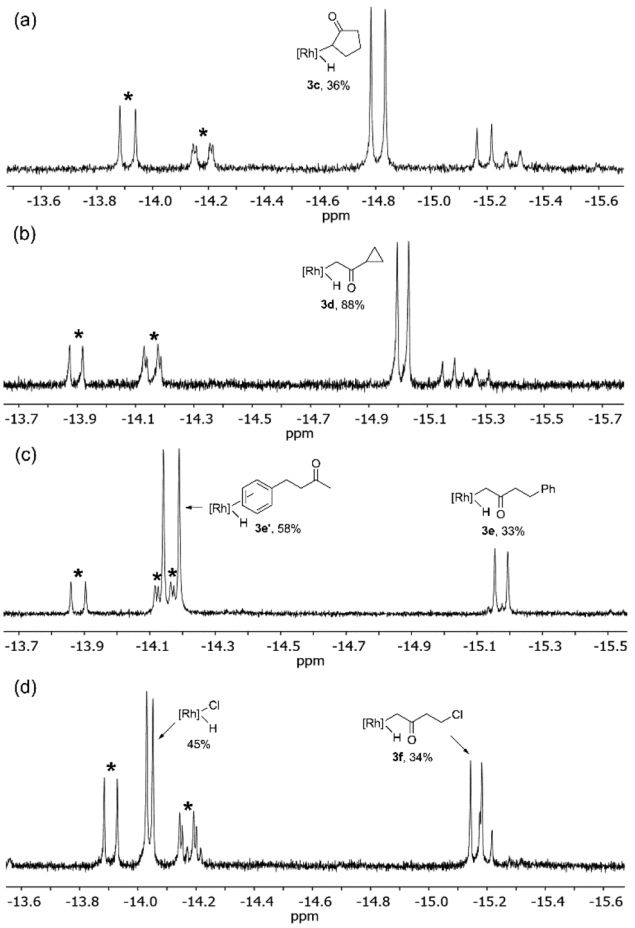

Fig. 3 ^{1}H NMR spectrum (500 MHz) of the hydride region of the reaction of **4** with (a) cyclopentanone, (b) methyl cyclopropyl ketone, and (c) 4-phenyl-2-butanone. All spectra recorded in C_6D_{12}. * indicates *o*-, *m*-, and *p*-carbodiimide activation products.

doublets (~5%) at δ −14.53 and −15.30 with $J_{Rh-H} \approx 22$ Hz, which could be attributed to diastereomers resulting from α-keto C–H activation, but their low abundance makes this assignment tentative (Fig. 2a). Attempts to isolate and characterize **3a** by treating with either CCl_4 or $CHBr_3$ were unsuccessful.

Interestingly, activation of methyl ethyl ketone results in the rapid formation of two major species **3b** and **3b′**. The larger hydride resonance at δ −14.79 (d, J_{Rh-H} = 20.5 Hz) is assigned to Tp′Rh(CNR)($CH_2C(O)CH_2CH_3$)(H) (**3b**). This small Rh–H coupling constant is typical for α-substituted alkyl hydride complexes.[16] Much like diethyl ketone activation, **3b′** is assigned to Tp′Rh(CNR)($CH_2CH_2C(O)CH_3$)(H) which features a hydride resonance at δ −14.90 (d, J_{Rh-H} = 24.0 Hz) with a larger coupling constant for activation of the β-methyl C–H bond. Also, two small doublets (~5%) are seen at δ −14.54 and −15.30 with $J_{Rh-H} \approx 23$ Hz that could arise from the diastereomers formed from α-ethyl C–H activation (Fig. 2b).

For higher boiling substrates that could not be readily removed under vacuum without heating, selectivity for C–H bond activation was investigated using the cyclohexyl deuteride derivative, Tp′Rh(CNneopentyl)(C_6D_{11})D, **4**, which serves as a thermal precursor to the reactive intermediate [Tp′Rh(CNneopentyl)]. Activation of cyclopentanone **2c** gave many C–H activated products alongside carbodiimide activation. The identity of the major product **3c** was assigned based on the coupling constant observed, J_{Rh-H} = 20.4 Hz, indicating α-keto C–H activation. Hydride resonances for additional minor C–H activation products appeared at δ −15.19 (J_{Rh-H} = 21.1 Hz) and δ −15.29 (J_{Rh-H} = 22.5 Hz). Presumably, these resonances correspond to either β-C–H activation of cyclopentanone or a diastereomer of the α-keto activation, although these assignments are tentative (Fig. 3a).

Activation of cyclopropyl methyl ketone **2d** *via* exchange with Tp′Rh(CNneopentyl)(C_6D_{11})(D) results in the formation of major product **3d** with a coupling constant of J_{Rh-H} = 19.5 Hz, indicative of C–H activation of the methyl group. The majority of the remaining mass balance was composed of carbodiimide C–H activation (Fig. 3b). Only traces of products that may indicate cyclopropyl C–H activation are seen (*c.f.* for activation of cyclopropane, ^{1}H NMR(C_6D_6): δ −14.89, d, J_{Rh-H} = 25 Hz).[18]

Irradiation of **1** in C_6D_{12} followed by exchange with 4-phenyl-2-butanone **2e** yields two major products. One hydride resonance at δ −15.17 (d, J_{Rh-H} = 19.5 Hz) indicates activation of the methyl group (**3e**). A second larger doublet is observed at δ −14.17 (J_{Rh-H} = 24.0 Hz) and is consistent with C–H activation of the phenyl group. The exact isomer of this oxidative addition product could not be readily identified, as activations of *o*-, *m*-, or *p*-C–H bonds are possible (Fig. 3c), yet only one doublet is observed.

Exchange of Tp′Rh(CNneopentyl)(C_6D_{11})(D) with 4-chloro-2-butanone (**2f**) led to the formation of methyl activation product **3f** which is accompanied by carbodiimide activation

Published on 27 May 2019. Downloaded by Nottingham Trent University on 6/6/2019 1:24:10 AM.

and an unexpected hydride resonance at δ −14.04 (d, J_{Rh-H} = 10.5 Hz) (Fig. 3d). The data for this latter product are very similar to those reported for Tp′Rh(CNneopentyl)HCl (−13.40, d, J = 11.5 Hz) in C_6D_6.[14] It is likely that the C_6D_{12} induces a solvent shift in the position of the resonance. Therefore, the chemical shift of Tp′Rh(CNneopentyl)HCl in C_6D_{12} was confirmed by photolysis of **1** and 2-chloropropane in C_6D_{12}. Formation of this product is consistent with α-keto activation followed by rapid β-chloride elimination, as observed with many other chloroalkanes.[14]

C–H activation of esters

Next, we sought to investigate the regioselectivity for C–H activation in the presence of ester containing substrates (Scheme 2 and Table 1, entries 8–12). ^{1}H NMR analysis of the photolysis of **1** in methyl acetate shows activation of both α-CH_3 (**3g**) and methoxy (**3g′**) C–H bonds (Fig. 4a). Tp′Rh(CNR)($CH_2C(O)OCH_3$)(H) (**3g**) shows a hydride resonance at δ −14.55 (d, J_{Rh-H} = 20.2 Hz) while **3g′** shows a hydride resonance at δ −14.50 (d, J_{Rh-H} = 24.1 Hz). Surprisingly, when the aliphatic chain length is extended as in methyl butyrate (**2h**), almost exclusive activation of the butyrate methoxy C–H bond (**3h**) is observed as a doublet at δ −14.54 with J = 23.9 Hz (Table 1, entry 10) (Fig. 4b). Additional evidence for this assignment is the long half-life for reductive elimination for this product (*vide infra*, $t_{1/2}$ = 37 h, *vs.* 12 h for an alkyl hydride product). Furthermore, photolysis of **1** in the presence of dimethyl carbonate produced the expected oxidative addition product **3i** at δ −14.24 (d, J_{Rh-H} = 24.1 Hz) as the sole product (Fig. 4c). The observed coupling constant is consistent with that of **3g′** and **3h**.

Substrates bearing C–Br bonds were investigated, however, no C–H activation products were observed by ^{1}H NMR spectroscopy (eqn (1)). Attempts to characterize the species formed by treating with bromoform yielded dibrominated species **5**. Lastly, C–H activation of aromatic ketones was attempted, but selectivity was poor and many aromatic C–H bonds alongside α-methyl activation were observed. Due to the many C–H

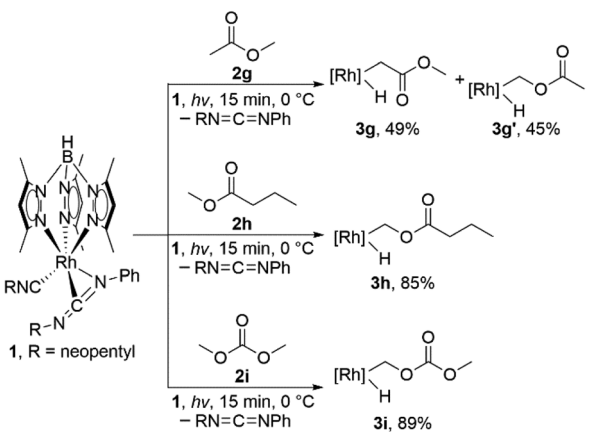

Scheme 2 Products from reaction of [Tp′Rh(CNR)] with various esters.

Table 1 Data for major products from the photolysis of **1** in various substrates[a]

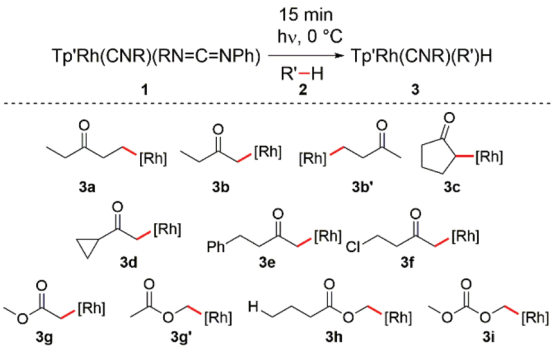

Entry	Product	3[b] (%)	Hydride resonance (δ)[c]	J_{Rh-H} (Hz)
1	**3a**	88	−14.89	24.0
2	**3b**	57	−14.79	20.5
3	**3b′**	37	−14.90	24.0
4	**3c**	36	−14.82[d]	20.4
5	**3d**	60	−15.02[d]	19.5
6	**3e**	33	−15.17[d]	19.5
7	**3f**	34	−15.16[d]	19.5
8	**3g**	49	−14.55	20.2
9	**3g′**	45	−14.50	24.1
10	**3h**	85	−14.54	23.9
11	**3i**	89	−14.24	24.1

[a] Samples were irradiated for 15 min at 0 °C. [b] Yields determined *via* integration of ^{1}H NMR spectra *vs.* hexamethyldisiloxane as an internal standard. [c] Hydride resonance reported in C_6D_6. [d] Hydride resonance reported in C_6D_{12}.

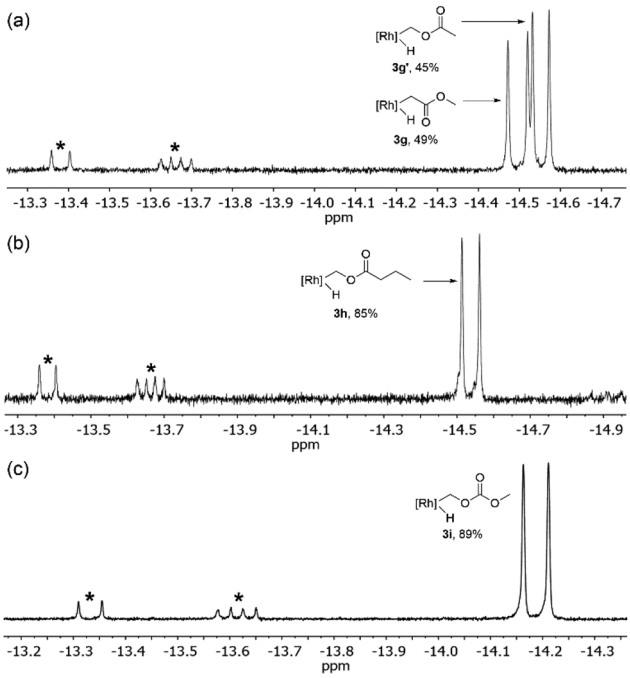

Fig. 4 ^{1}H NMR spectrum (500 MHz) of the hydride region of the reaction of esters with **1**: (a) methyl acetate, (b) methyl butyrate, and (c) dimethylcarbonate. All spectra recorded in C_6D_6. * indicates *o*-, *m*-, and *p*-carbodiimide activation products.

This journal is © The Royal Society of Chemistry 2019

Published on 27 May 2019. Downloaded by Nottingham Trent University on 6/6/2019 1:24:10 AM.

bonds activated, analysis of these reaction mixtures was challenging and not pursued. Table 1 summarizes the data for the reactions of all ketones and esters with **1**.

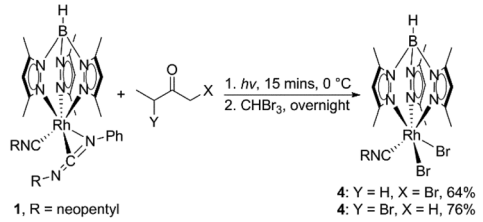

(1)

Kinetics of reductive eliminations

Rates for the reductive elimination of Tp′Rh(CNneopentyl)(R)(H) complexes in either C_6D_6 or C_6D_{12} were determined by monitoring the first-order disappearance of the Rh–H resonance by ^{1}H NMR spectroscopy (Table 2). Reductive elimination of α-substituted alkyl hydride complex **3b** was slower when compared to **3a** and **3b′** at room temperature. Reductive elimination of methoxy activated C–H bond in **3g′** was 2.4× times faster than α-substituted **3g** at 60 °C. This suggests that α substitution provides additional stability to the resulting hydride complex. While extending the aliphatic chain length in **3h** (compared to **3g′**) results in near exclusive methoxy C–H activation, the rate of reductive elimination of methyl butyrate from **3h** is similar to that of methyl acetate from **3g′** at 60 °C. In contrast, reductive elimination of dimethyl carbonate from **3i** is slow ($t_{1/2}$ = 111.13 h), showing a strong electronic effect of the carbonate.

The reductive elimination of 4-chloro-2-butanone from **3f** was conducted at room temperature and a rate of 8.21 (46) × 10^{-6} s^{-1} was observed. However for 4-phenyl-2-butanone, elevated temperature was necessary to observe an appreciable decrease in the corresponding hydride resonance. Reductive elimination of methyl cyclopropyl ketone from **3d** also required elevated temperature and was faster than 4-phenyl-2-butanone reductive elimination from **3e**. Lastly, reductive elimination of cyclopentanone from **3c** at 40 °C was relatively fast, suggesting that sterics associated with a secondary carbon–rhodium bond may play a factor in thermodynamic stability.

Table 2 Rates of reductive elimination of ketones and esters from Tp′Rh(CNR)(R)(H) (**3a–3i**) in C_6D_6 [a]

Product	T (°C)	k_{re} (s^{-1})	$t_{1/2}$ (h)	$\Delta G^{\ddagger}_{re}$ (kcal mol^{-1})
$CH_2C(=O)CH_3$	70	1.11 (2) × 10^{-5}	17.3	27.71 (1)
3a	24	1.65 (7) × 10^{-5}	11.70	23.88 (3)
3b	24	9.51 (54) × 10^{-7}	202.42	25.57 (3)
3b′	24	1.78 (6) × 10^{-5}	10.82	23.84 (2)
3c	40	1.03 (1) × 10^{-5}	18.67	25.49 (1)
3d	70	7.74 (52) × 10^{-6}	24.88	28.19 (5)
3e	70	5.35 (12) × 10^{-6}	36.00	28.45 (2)
3f	24	8.21 (46) × 10^{-6}	23.45	24.29 (3)
3g	60	2.13 (3) × 10^{-6}	90.38	28.21 (1)
3g′	60	5.08 (12) × 10^{-6}	37.86	27.63 (2)
3h	60	5.21 (12) × 10^{-6}	36.98	27.61 (2)
3i	60	1.73 (2) × 10^{-6}	111.13	28.34 (1)

[a] Errors are reported as standard deviation. Errors in $\Delta G^{\ddagger}_{re}$ are calculated from k as propagated errors, using $\sigma_G = (RT/k_{re})\sigma_k$. The errors are small because G is a log function of rate. Systematic errors are probably larger and can be estimated as ±0.1 kcal mol^{-1} assuming 10% error in k. Substrates **2c–f** in C_6D_{12}.

Competitive kinetic selectivities

Next, the relative selectivity of the coordinatively unsaturated fragment [Tp′Rh(CNneopentyl)] for C–H bond activation was determined in a mixture of two substrates (Table 3). Samples were irradiated for a short time so that the product ratio represents the kinetic products of the reaction mixture. The relative competitive rates (k_2/k_1) were determined on the basis of the relative areas of the corresponding resonances by ^{1}H NMR spectroscopy using eqn (2), where I_2/I_1 is the integration area of the hydride resonances and n_1/n_2 is the mole ratio of the two substrates in question (subscript 1 refers to the competing substrate and subscript 2 refers to benzene). Furthermore, the difference in free energies of activation $\Delta\Delta G^{\ddagger}_{oa}$ can be calculated using eqn (3).

Since reductive elimination experiments were conducted at varying temperatures (Table 2), the $\Delta G^{\ddagger}$ for benzene reductive elimination at each respective temperature was calculated using known activation parameters.[17] Combining $\Delta G^{\ddagger}_{re}$ for benzene, $\Delta G^{\ddagger}_{re}$ for the substrate of interest, and $\Delta\Delta G^{\ddagger}_{oa}$, ΔG° can be calculated (eqn (4), Table 4). Finally, the relative Rh–C bond strengths of C–H activated substrates compared to D(Rh–Ph) were calculated using eqn (5), which includes the assumption that $\Delta G^{\circ} = \Delta H^{\circ} - RT\ln(H/H')$, where H/H' is the ratio of the number of available hydrogen atoms on the

Table 3 Kinetic selectivity data determined from competition experiments[a]

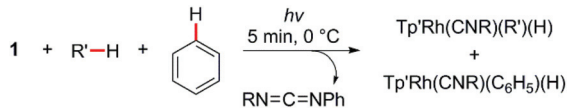

Entry	Substrates	k_2/k_1 [b]	$\Delta\Delta G^{\ddagger}_{oa}$ [c] (kcal mol^{-1})
1[d]	Benzene: acetone	3.71 (19)	0.73 (3)
2	Benzene: **2a**	1.37 (7)	0.19 (3)
3	Benzene: **2b**	1.97 (10)	0.40 (3)
4	Benzene: **2b′**	1.76 (9)	0.34 (3)
5	Benzene: **2c**	20.85 (104)	1.79 (3)
6	Benzene: **2d**	10.06 (50)	1.36 (3)
7	Benzene: **2e**	2.44 (12)	0.53 (3)
8[e]	Benzene: **2f**	—	—
9	Benzene: **2g**	6.11 (31)	1.07 (3)
10	Benzene: **2g′**	7.51 (38)	1.19 (3)
11	Benzene: **2h**	17.36 (87)	1.68 (3)
12	Benzene: **2i**	3.21 (15)	0.69 (3)

[a] Each sample was irradiated for 5 minutes at 0 °C. [b] Errors in rate ratio estimated at 5% for proton NMR integrations, giving $\sigma_G = (RT/\text{ratio})\sigma_{ratio} = 0.05RT \approx 0.03$ kcal mol^{-1}. [c] A positive value denotes that benzene is kinetically favored. [d] Irradiation done at 8 °C, see ref. 9. [e] Attempts to obtain kinetic selectivity data for 4-chloro-2-butanone were unsuccessful.

Published on 27 May 2019. Downloaded by Nottingham Trent University on 6/6/2019 1:24:10 AM.

Table 4 Kinetic and thermodynamic data for Tp′Rh(CNneopentyl)(R)(H)[a]

Product	No. of H	$\Delta\Delta G^{\ddagger}_{oa}$	ΔG° [b]	D(R–H)[c]	D_{rel}(Rh–C)[e]
Phenyl	6	0.00	0.00 (5)	112.9[d]	0.00
$CH_2C(=O)CH_3$	6	0.71 (3)	0.21 (9)	96.00	−17.1
3a	6	0.17 (3)	3.97 (11)	98.34	−18.5
3b	3	0.31 (3)	2.42 (11)	91.34	−23.6
3b′	3	0.37 (3)	4.21 (10)	98.94	−17.8
3c	4	1.65 (3)	3.67 (9)	85.34	−31.0
3d	3	1.25 (3)	0.27 (13)	91.22	−21.5
3e	3	0.48 (3)	−0.76 (10)	90.22	−21.5
3f	3	—	—	90.67	—
3g	3	0.98 (3)	0.08 (9)	93.59	−19.0
3g′	3	1.09 (3)	0.77 (10)	95.95	−17.3
3h	3	1.55 (3)	1.25 (10)	94.63	−19.1
3i	6	0.63 (3)	−0.040 (9)	96.83	−15.7

[a] All values are in kcal mol^{-1}. [b] Error is the summation of the individual errors in associated with eqn (3). [c] C–H bond strengths were calculated using B3LYP/6-311g. [d] Benzene C–H bond strength is from ref. 23. [e] D_{rel}(Rh–H) as defined in eqn (5) refers to the Rh–C bond strength relative to the Rh–Ph bond strength.

substrates. This accounts for the statistical contribution to the free energy.

$$\frac{k_2}{k_1} = \left(\frac{I_2}{I_1}\right)\left(\frac{n_1}{n_2}\right) \quad (2)$$

$$\Delta\Delta G^{\ddagger}_{oa} = RT\ln\left(\frac{k_2}{k_1}\right) \quad (3)$$

$$\Delta G^{\circ} = \Delta G^{\ddagger}_{re}(\text{R'H}) + \Delta\Delta G^{\ddagger}_{oa} - \Delta G^{\ddagger}_{re}(\text{PhH}) \quad (4)$$

$$\begin{aligned} D_{rel}(\text{Rh–C}) &= [\Delta H(\text{Rh–R}) - \Delta H(\text{Rh–Ph})] \\ &= [D(\text{R–H}) - D(\text{Ph–H})] - \Delta G^{\circ} \\ &\quad + RT\ln\left(\frac{6}{\#\text{H}}\right) \end{aligned} \quad (5)$$

A plot of the relative Rh–C bond strengths *vs.* the C–H bond strengths shows a linear correlation for the studied substrates with α-keto or α-O_2CR substitutions (Fig. 5). The positive correlation indicates that the Rh–C bond strengths could be inferred from the corresponding C–H bond strengths in R–H. The observed slope, $R_{M-C/C-H}$ = 1.22 (12), suggests that the Rh–C bond strengths vary in proportion to the C–H bond strengths, as was seen in the case of related systems where $R_{M-C/C-H}$ is also larger than unity (~1.4).[16,19,20]

All of the products in these reactions except for two (plus benzene) possess either α-keto or –CH_2OR functional groups. The two data points with β-keto groups with D(C–H) ≈ 98 kcal mol^{-1} and benzene are seen to lie on a slightly lower line with $R_{M-C/C-H}$ = 1.27 (1), as would be expected for activation of a C–H bond with no α-substitution.[16]

Of note here is the kinetic preference for terminal methyl C–H bond activation even though α-keto C–H activation is expected to be thermodynamically preferred. The observation of only trace quantities of resonances that could be attributed to the latter are consistent with the general observation that

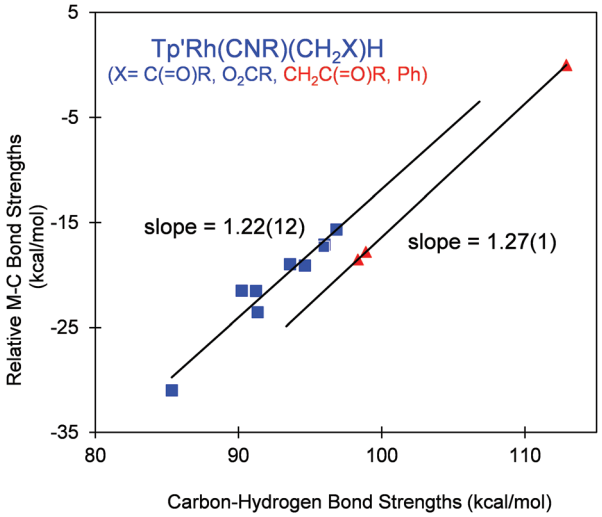

Fig. 5 Plot of relative experimental M–C bond strengths *vs.* C–H bond strengths for Tp′Rh(CNneopentyl)(R)(H). Hydrocarbon C–H bond strengths were calculated using B3LYP/6-311g. Blue squares refer to α-keto or α-O functionalized Rh–CH_2X products. Red triangles refer to β-keto Rh–$CH_2CH_2C(=O)$R and phenyl products.

activation of CH_2 bonds is kinetically slow. Consequently, in alkyl ketones and esters methyl C–H activation strongly predominates.

Conclusions

Photolysis of Tp′Rh(CNneopentyl)(PhNCNneopentyl) **1** in the presence of aliphatic ketones and esters results in C–H activation products of the type Tp′Rh(CNneopentyl)(R)(H) **3**, where reactions of methyl groups dominate the observed products. Only traces of secondary, α-keto CH_2 activation are observed. The reductive elimination of RH from Tp′Rh(CNneopentyl)(R)(H) in C_6D_6 or C_6D_{12} was monitored and in combination with competition experiments allowed for the determination of the relative Rh–C bond strengths. In general, C–H activation products containing α-substituents provide additional stability to the resulting hydride species. While α-ester substituents do provide additionally stability, α-keto substituents result in stronger Rh–C bonds. A positive correlation $R_{Rh-C/C-H}$ = 1.22 was observed suggesting that the relative Rh–C bond strength can be inferred directly from the relative C–H bond strength in this class of substrates.

Materials and methods

General procedures

All operations and routine manipulations were performed under a nitrogen atmosphere or on a high-vacuum line using modified Schlenk techniques. Diethyl ketone, ethyl methyl ketone, methyl acetate, methyl butyrate, dimethyl carbonate, 4-phenyl-2-butanone, 4-hydroxy-2-butanone, cyclopropyl methyl ketone, cyclopentanone, carbon tetrachloride, and bro-

This journal is © The Royal Society of Chemistry 2019

Published on 27 May 2019. Downloaded by Nottingham Trent University on 6/6/2019 1:24:10 AM.

moform were purchased from Sigma Aldrich. The synthesis of 4-chloro-2-butanone has been previously reported.[21] Benzene-d_6 (Cambridge Isotopes) was distilled under vacuum from a dark purple solution of benzophenone ketyl and stored in a Schlenk flask under nitrogen atmosphere. Cyclohexane-d_{12} (Cambridge Isotopes) was degassed by three freeze–pump–thaw cycles and stored over activated 3 Å molecular sieves. Other solvents were used directly from an Innovative Technologies PS-MD-6 solvent system. The synthesis of Tp′Rh(CNneopentyl)(PhNCN-neopentyl) (**1**) has been previously reported.[22]

All photolysis experiments were performed using a 200 W Hg(Xe) arc lamp purchased from Oriel, which was fitted with a water-filled IR filter and a 324 nm high pass filter. All experiments were performed at 0 °C. All ^{1}H and ^{13}C NMR spectra were collected on either a Bruker Avance 400 or Avance 500 MHz spectrometer. Chemical shifts are reported in ppm (δ) referenced to the residual solvent peaks of C_6D_6 (δ = 7.16) and C_6D_{12} (δ = 1.38). Elemental analysis was performed by the University of Rochester using a PerkinElmer 2400 series II elemental analyzer in CHN mode. All kinetic plots and least-square error analysis were done using Microsoft Excel.

Reactions in benzene-d_6

Reactions were setup in a nitrogen filled glovebox. To an oven-dried 5 mm J Young NMR tube was added **1** (6.9 mg, 0.010 mmol). Next, 0.5 mL the corresponding R–H substrate was added and the NMR tube was capped. The sample was removed from the glovebox and irradiated at 0 °C for 15 min. After 15 min, the reaction was removed from the ice bath and the excess substrate was removed *in vacuo*. The resulting residue was dissolved in C_6D_6, heated if necessary, and the disappearance of the hydride resonance was monitored over time by ^{1}H NMR spectroscopy.

Reactions in cyclohexane-d_{12}

Reactions were setup in a nitrogen filled glovebox. To an oven-dried 5 mm J Young NMR tube was added **1** (6.9 mg, 0.010 mmol). Next, 1 drop the corresponding R–H substrate was added followed by 0.5 mL of C_6D_{12}. The NMR tube was capped and the sample was removed from the glovebox and irradiated at 0 °C for 15 min. After 15 min, the reaction was removed from the ice bath and heated if necessary. The disappearance of the hydride resonances was monitored over time by ^{1}H NMR spectroscopy.

Conflicts of interest

The authors declare no competing financial interest.

Acknowledgements

The authors gratefully acknowledge funding from the U.S. Department of Energy (Grant. No. FG02-86ER-13569) for instrumentation and chemicals, and the NSF for a Graduate Fellowship (DGE-1419118 to A. M. P.). Andrew VanderWeide is acknowledged for assistance with DFT calculations.

Notes and references

1 (*a*) J. Wencel-Delord and F. Glorius, *Nat. Chem.*, 2013, **5**, 369–375; (*b*) D. J. Abrams, P. A. Provencher and E. J. Sorensen, *Chem. Soc. Rev.*, 2018, **47**, 8925–8967.

2 (*a*) A. H. Janowicz and R. G. Bergman, *J. Am. Chem. Soc.*, 1983, **105**, 3929–3939; (*b*) J. M. Buchanan, J. M. Stryker and R. G. Bergman, *J. Am. Chem. Soc.*, 1986, **108**, 1537–1550; (*c*) M. J. Wax, J. M. Stryker, J. M. Buchanan, C. A. Kovac and R. G. Bergman, *J. Am. Chem. Soc.*, 1984, **106**, 1121–1122; (*d*) W. D. Jones and F. J. Feher, *J. Am. Chem. Soc.*, 1984, **106**, 1650–1663; (*e*) W. D. Jones and F. J. Feher, *Acc. Chem. Res.*, 1989, **22**, 91–100.

3 (*a*) S. P. Nolan, C. D. Hoff, P. O. Stoutland, L. J. Newman, J. M. Buchanan, R. G. Bergman, G. K. Yang and K. S. Peters, *J. Am. Chem. Soc.*, 1987, **109**, 3143–3145; (*b*) J. Halpern, *Inorg. Chim. Acta*, 1985, **100**, 41–48; (*c*) E. P. Wasserman, C. B. Moore and R. G. Bergman, *Science*, 1992, **255**, 315–318; (*d*) J. A. M. Simões and J. L. Beauchamp, *Chem. Rev.*, 1990, **90**, 629–688; (*e*) C. P. Schaller, C. C. Cummins and P. T. Wolczanski, *J. Am. Chem. Soc.*, 1996, **118**, 591–611.

4 W. D. Jones and E. T. Hessell, *J. Am. Chem. Soc.*, 1993, **115**, 554–562.

5 J. L. Bennett and P. T. Wolczanski, *J. Am. Chem. Soc.*, 1997, **119**, 10696–10719.

6 C. P. Schaller and P. T. Wolczanski, *Inorg. Chem.*, 1993, **32**, 131–144.

7 A. R. Bulls, J. E. Bercaw, J. M. Manriquez and M. E. Thompson, *Polyhedron*, 1988, **7**, 1409–1428.

8 H. E. Bryndza, L. W. Fong, R. A. Paciello, W. Tam and J. E. Bercaw, *J. Am. Chem. Soc.*, 1987, **109**, 1444–1456.

9 L. E. Schock and T. J. Marks, *J. Am. Chem. Soc.*, 1988, **110**, 7701–7715.

10 E. Clot, C. Mégret, O. Eisenstein and R. N. Perutz, *J. Am. Chem. Soc.*, 2006, **128**, 8350–8257.

11 (*a*) E. Clot, M. Besora, F. Maseras, C. Mégret, O. Eisenstein, B. Oelckers and R. N. Perutz, *Chem. Commun.*, 2003, 490–491; (*b*) E. Clot, B. Oelckers, A. H. Klahn, O. Eisenstein and R. N. Perutz, *Dalton Trans.*, 2003, 4065–4074; (*c*) E. Clot, C. Mégret, O. Eisenstein and R. N. Perutz, *J. Am. Chem. Soc.*, 2009, **131**, 7817–7827.

12 J. Uddin, C. M. Morales, J. H. Maynard and C. R. Landis, *Organometallics*, 2006, **25**, 5566–5581.

13 A. J. Vetter and W. D. Jones, *Polyhedron*, 2014, **23**, 413–417.

14 A. J. Vetter, R. D. Rieth, W. W. Brennessel and W. D. Jones, *J. Am. Chem. Soc.*, 2009, **131**, 10742–10752.

15 A. J. Vetter, R. D. Rieth and W. D. Jones, *Proc. Natl. Acad. Sci. U. S. A.*, 2007, **104**, 6957–6962.

16 Y. Jiao, M. E. Evans, J. Morris, W. W. Brennessel and W. D. Jones, *J. Am. Chem. Soc.*, 2013, **135**, 6994–7004.
17 W. D. Jones and E. T. Hessell, *J. Am. Chem. Soc.*, 1992, **114**, 6087–6095.
18 D. D. Wick, T. O. Northcutt, R. J. Lachicotte and W. D. Jones, *Organometallics*, 1998, **17**, 4484–4492.
19 Y. Jiao, J. Morris, W. W. Brennessel and W. D. Jones, *J. Am. Chem. Soc.*, 2013, **135**, 16198–16212.
20 Y. Jiao, W. W. Brennessel and W. D. Jones, *Chem. Sci.*, 2014, **5**, 804–812.
21 R. C. Simon, B. Grischek, F. Zepeck, A. Steinreiber, F. Belaj and W. Kroutil, *Angew. Chem., Int. Ed.*, 2012, **51**, 6713–6716.
22 E. T. Hessell and W. D. Jones, *Organometallics*, 1992, **11**, 1496–1505.
23 Y.-R. Luo, *Comprehensive Handbook of Chemical Bond Energies*, CRC Press, Boca Raton, FL, 2007.

Published on 27 May 2019. Downloaded by Nottingham Trent University on 6/6/2019 1:24:10 AM.

This journal is © The Royal Society of Chemistry 2019